Quantum signatures of chaos in the dynamics of a trapped ion

J. K. Breslin,[1] C. A. Holmes,[2] and G. J. Milburn[1]

[1]*Department of Physics, The University of Queensland, St. Lucia, Queensland 4072, Australia*
[2]*Department of Mathematics, The University of Queensland, St. Lucia, Queensland 4072, Australia*
(Received 31 October 1996)

We show how a nonlinear chaotic system, the parametrically kicked nonlinear oscillator, may be realized in the dynamics of a trapped, laser-cooled ion, interacting with a sequence of standing-wave pulses. Unlike the original optical scheme [G. J. Milburn and C. A. Holmes, Phys. Rev. A **44**, 4704 (1991)], the trapped ion enables strongly quantum dynamics with minimal dissipation. This should permit an experimental test of one of the quantum signatures of chaos: irregular collapse and revival dynamics of the average vibrational energy. [S1050-2947(97)08109-2]

PACS number(s): 42.50.Vk, 05.45.+b, 42.50.Md

I. INTRODUCTION

It is now well understood that the quantum dynamics of a classically chaotic system will show major departures from the classical motion on a suitable time scale [1,2]. Systems that classically show chaotic diffusion of a slow momentum-like variable will cease to show diffusion after the "break time." In this region, the momentum distribution is found to be exponentially localized rather than Gaussian. One system that demonstrates this phenomenon is a laser-cooled atom moving under the dipole force of a standing wave with periodically modulated nodal positions [3,4]. Recently, this prediction achieved experimental confirmation in the work of Moore *et al.* [5]. The quantum and classical dynamics can also differ through the existence of quantum tunneling between fixed points of the classical Poincaré section, a phenomenon that has not yet been observed. In this paper we consider yet another way in which quantum and classical motion can differ for systems that classically do not show diffusion. In this case the transition to chaos in the classical system is manifested in the quantum case by a transition from regular collapse and revivals of average values with time to a highly irregular collapse and revival sequence [2(b)]. An example of such a system is the parametrically kicked nonlinear oscillator [6]. A nonlinear oscillator, in which the frequency is linearly dependent on energy, is periodically kicked by a parametric amplification process, which momentarily turns the origin into a hyperbolic fixed point. The classical dynamics of this system exhibits regions of regular and chaotic motion in the Poincaré section.

In Ref. [6] it was proposed to realize this system using a combination of a Kerr optical nonlinearity and an optical parametric amplifier. Unfortunately, the required optical nonlinearity is usually rather small and accompanied by a large amount of dissipation. For this reason, it is unlikely that an optical version will ever show interesting quantum features. However, the system does show some interesting classical chaotic behavior including a strange attractor in which unstable periodic orbits can be stabilized by Ott-Grebogi-Yorke control [7]. In this paper we show that a much more promising realization of the quantum version of this system may be achieved in the dynamics of a single trapped laser-cooled ion interacting with a sequence of pulsed optical fields. Furthermore, the dynamics may be monitored with high quantum efficiency using the quantum nondemolition (QND) vibrational energy measurement scheme proposed by de Matos Filho and Vogel [8] together with the now standard method of detection on a strong probe transition.

We consider the vibrational motion of a single trapped ion. In the absence of laser pulses, the ion executes simple harmonic motion in the quadratic trap potential. As we show below, a suitable sequence of laser pulses enables us to realize the nonlinear quantum dynamics specified by the map

$$|\psi_{n+1}\rangle = U_{NL}U_{PA}|\psi_n\rangle, \tag{1}$$

where

$$U_{NL} = \exp\left(-i\theta a^\dagger a - i\frac{\mu}{2}(a^\dagger)^2 a^2\right) \tag{2}$$
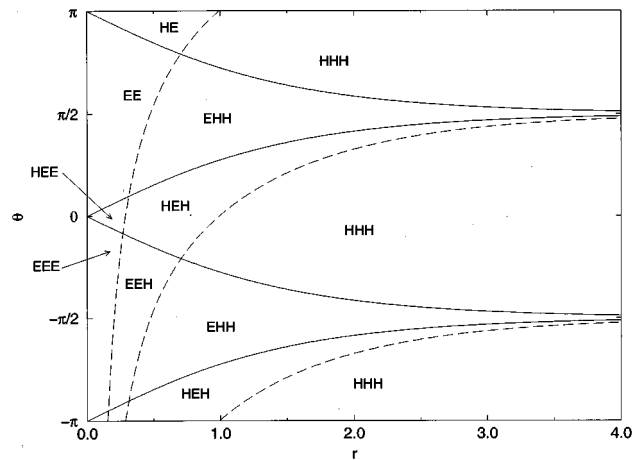

FIG. 1. Bifurcation diagram for the origin and the period-1 orbits close to the origin. The bifurcation curves for the origin are represented as solid lines, while those for the period-1 orbits are dashed. The regions are labeled by a finite sequence of *E*'s and *H*'s, standing for elliptic and hyperbolic. The first letter refers to the stability of the origin, the second to that of the pair of period-1 orbits closest to the origin in the second and fourth quadrants (those in the first and third are always hyperbolic), the third to the pair of period-1 orbits next closest to the origin, etc.

describes an intensity-dependent rotation in the oscillator phase plane, while

$$U_{PA} = \exp\left(\frac{r}{2}[(a^\dagger)^2 - a^2]\right) \tag{3}$$

describes a parametric amplification kick. In these expressions the operators $a, a^\dagger$ are the ladder operators for the quantized harmonic motion of the trapped ion, which may be written in terms of the dimensionless position and momentum operators $\hat{X}_1, \hat{X}_2$ as $a = \hat{X}_1 + i\hat{X}_2$.

II. CLASSICAL DYNAMICS

The classical model corresponding to Eq. (1) is closely related to the model in Ref. [6],

$$X'_1 = g[\cos(\theta + \mu R^2)X_1 + \sin(\theta + \mu R^2)X_2], \tag{4}$$

$$X'_2 = \frac{1}{g}[\cos(\theta + \mu R^2)X_2 - \sin(\theta + \mu R^2)X_1], \tag{5}$$

where $R^2 = X_1^2 + X_2^2$ and the parametric gain is $g = e^r$. The parameter μ is simply a scaling parameter and the crucial control parameters are the parametric gain g and θ. When $\theta = 2\pi$, easily achievable in experiment as we show below, this model reduces to that discussed in Ref. [6]. The origin is then a saddle. If, however, $|\cosh r \cos\theta| < 1$, where $r = \ln g$, the origin is elliptically stable. The bifurcation diagram is shown in Fig. 1. The origin is elliptically stable in the regions bounded by the solid curves $\theta = \pm \arccos(1/\cosh r) + n\pi$ and labeled $E**$. Away from the origin an infinite number of period-1 orbits lie on lines with a slope of $\pm e^{(-r)}$, independent of θ as in the original model. However, the radius at which the period-1 orbits lie does depend on θ and is determined by the equation

$$-\tan(\theta + \mu R^2) = \pm \sinh r. \tag{6}$$

As θ is increased the period-1 orbits move inward, collapsing on the origin and changing its stability. Those in the odd
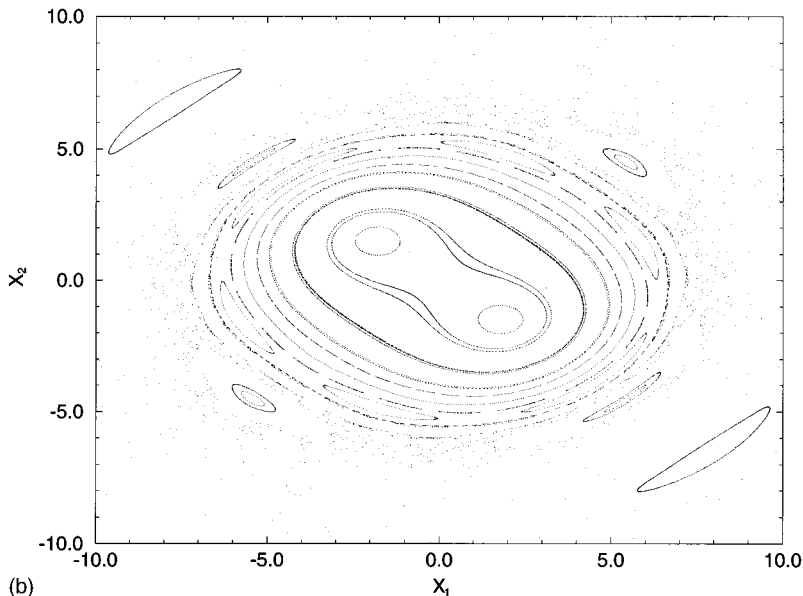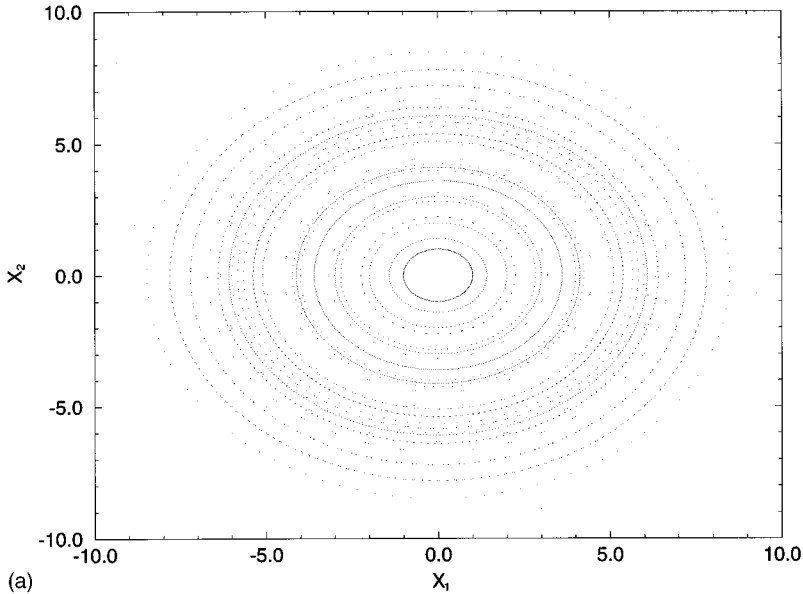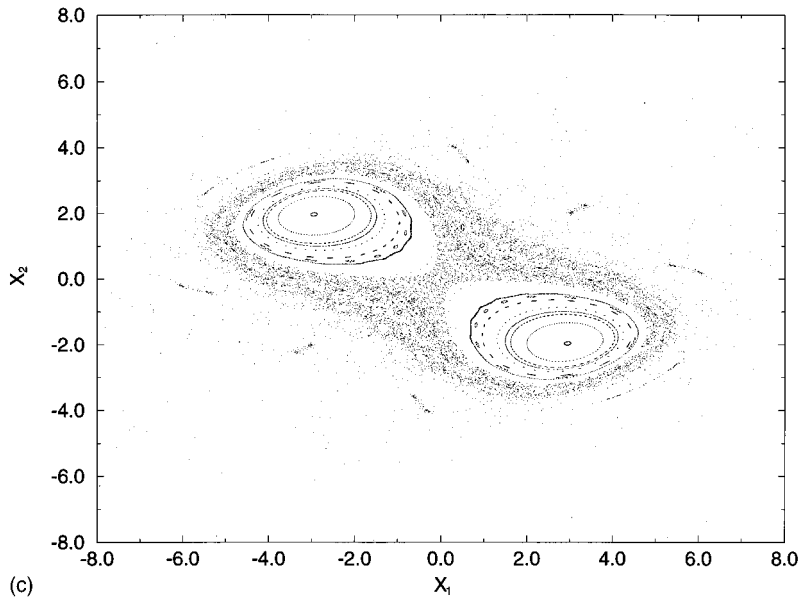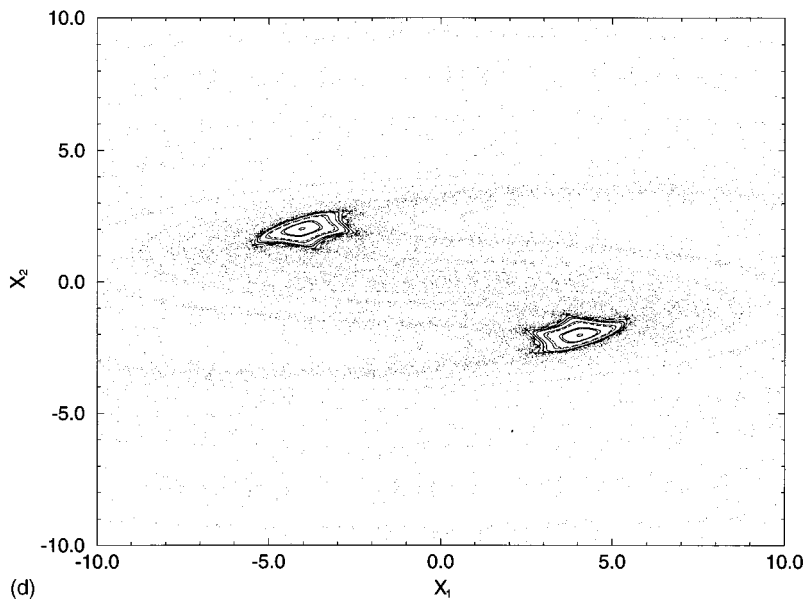

(a)

(b)

FIG. 2. Phase-space portraits for the classical map. In all cases $\mu = 0.01\pi$ and $\theta = 2\pi$. (a) $g = 1.0$, (b) $g = 1.2$, (c) $g = 1.5$, and (d) $g = 2.0$.

FIG. 2 (*Continued*).

quadrants are always unstable. In the even quadrants a finite number (maybe zero) lying closest to the origin are stable depending on whether

$$1 > \mu R^2 \tan(\theta + \mu R^2) > 0. \tag{7}$$

They lose stability on the curves $\theta = \arctan(\sinh r) - 1/\sinh r + n\pi$, shown as dashed (for $n = -1, 0, 1$) in Fig. 1. The various parameter regions are labeled with a sequence of E's and H's standing for elliptic or hyperbolic. The first letter refers to the stability of the origin and the subsequent letters to the stability of the pairs of period-1 orbits in the second and fourth quadrants starting with those closest to the origin and moving out. Since the elliptic period-1 orbits always occur closest to the origin in the region EEH, for instance, only one pair of period-1 orbits is elliptically stable.

In Fig. 2 we show typical Poincaré sections of the classical dynamics for various values of g and $\theta = 2\pi$. Note the transition to almost global chaos for large values of g.

III. QUANTUM DYNAMICS

To compare the quantum and classical dynamics we compute the mean energy as a function of the number of kicks. In the quantum case we assume that the oscillator is initially prepared in the vibrational ground state, while in the classical case we use an initial Gaussian phase-space distribution with the same moments as the initial quantum state. The detailed results are given in Ref. [6], which we summarize here. In the classical case, the average energy saturates at an almost time-independent value, as the initial distribution becomes spread around the period-1 fixed points. The time taken to reach the saturation value is longer for an initial state in the regular region than for one located in a chaotic region. In the quantum case, the mean energy follows the classical for a short time, but instead of saturating at an almost stationary value it continues to oscillate with a characteristic collapse and revival envelope. The transition from regular to chaotic dynamics in the classical system is marked in the quantum system by a transition from a regular collapse
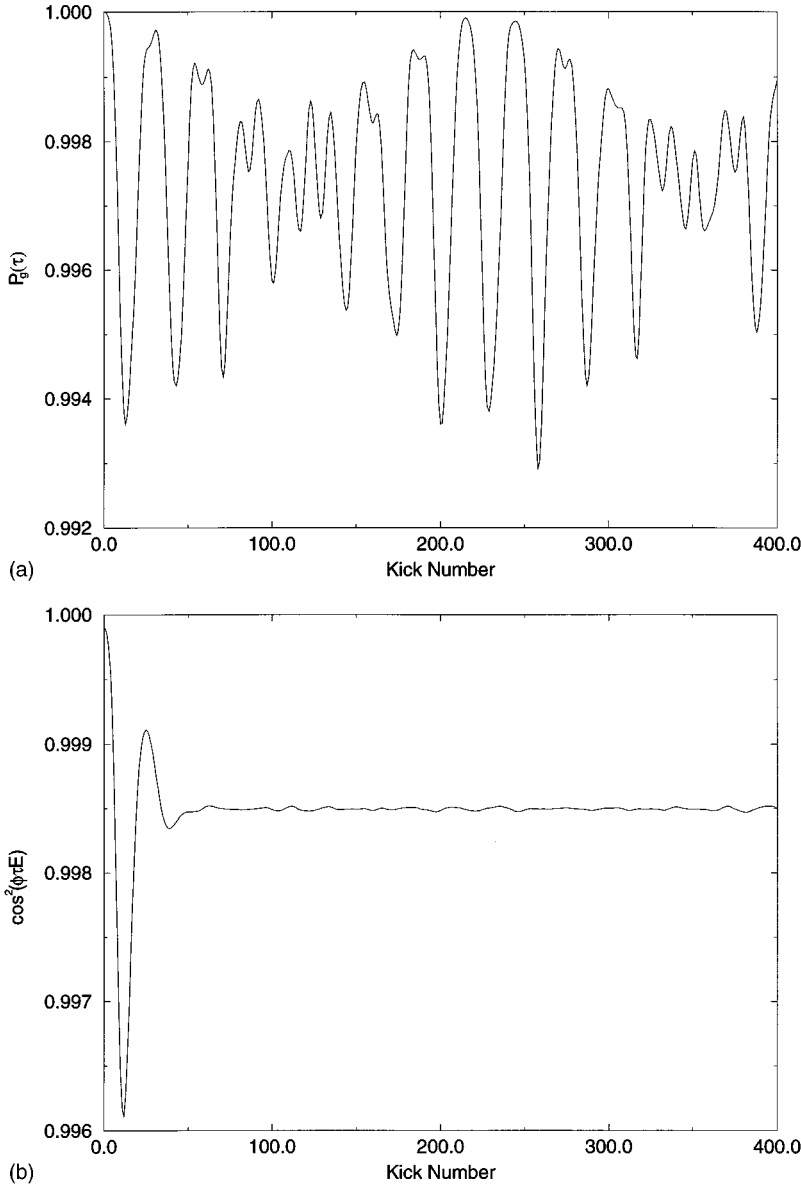
FIG. 3. Initial states centered in a classically regular region: (a) plot of the quantum average $P_g(\tau)=\langle\cos^2\phi\hat{m}\rangle$ for an initial coherent state and (b) plot of $\cos^2(\phi\tau E)$ (where E is the classical mean energy) for an initial Gaussian distribution. In both cases the initial state is centered at (0,0), with $g=1.2$, $\mu=0.01\pi$, $\theta=2\pi$, and $\phi\tau=0.01$.

and revival sequence to a highly irregular and more rapid collapse and revival sequence. This is due to the fact that a state localized in the chaotic region has support on many quasienergy eigenstates compared to a state localized in a regular region.

We now show how this system may be realized in a trapped ion experiment. Following de Matos Filho and Vogel [8], we first consider an ion trapped at an antinode of an optical standing wave tuned to the atomic frequency, the carrier frequency. In an interaction picture at frequency ν the interaction Hamiltonian is

$$H_I=-\hbar\Omega\,\eta^2 a^\dagger a\sigma_x+\hbar\,\frac{\Omega\,\eta^4}{4}(a^\dagger)^2 a^2\sigma_x, \qquad (8)$$

where Ω is the Rabi frequency and η is the Lamb-Dicke parameter. If the ion is first prepared in an eigenstate of σ_x by the application of a $\pi/2$ pulse, it will remain in this state. In that case the vibrational motion experiences a linear and a nonlinear phase shift. The interaction is precisely the kind

required to realize U_{NL}, with $\theta=T\Omega\,\eta^2$ and $\mu=T\Omega\,\eta^4/2$, where T is the time for which the standing-wave pulse is applied.

In order to realize the parametric kick we use a Raman interaction with two laser pulses, one tuned to the first lower sideband, the other to the first upper sideband. This scheme has been used successfully by Meekhof et al. to prepare the ion in a squeezed vibrational state [9]. In this case the interaction Hamiltonian, in an interaction picture at frequency ν, is

$$H_{PA}=i\hbar\,\kappa[a^2-(a^\dagger)^2], \qquad (9)$$

where $\kappa=\Omega_1\Omega_2\,\eta_R^2/8\delta_1\delta_2$ and Ω_i is the Rabi frequency for each of the Raman pulses, each of which is detuned from the atomic transition by δ_i such that $\delta_1-\delta_2=2\nu$. The Lamb-Dicke parameter for the Raman transition is $\eta_R=\delta kx_0$, where δk is the wave-vector difference for the two Raman beams and x_0 is the rms fluctuations of position in the ground state of the trap. Note that this Hamiltonian is independent of the ion electronic state. The ion evolves according to the parametric kick transformation with $g=e^{\kappa T}$ for a
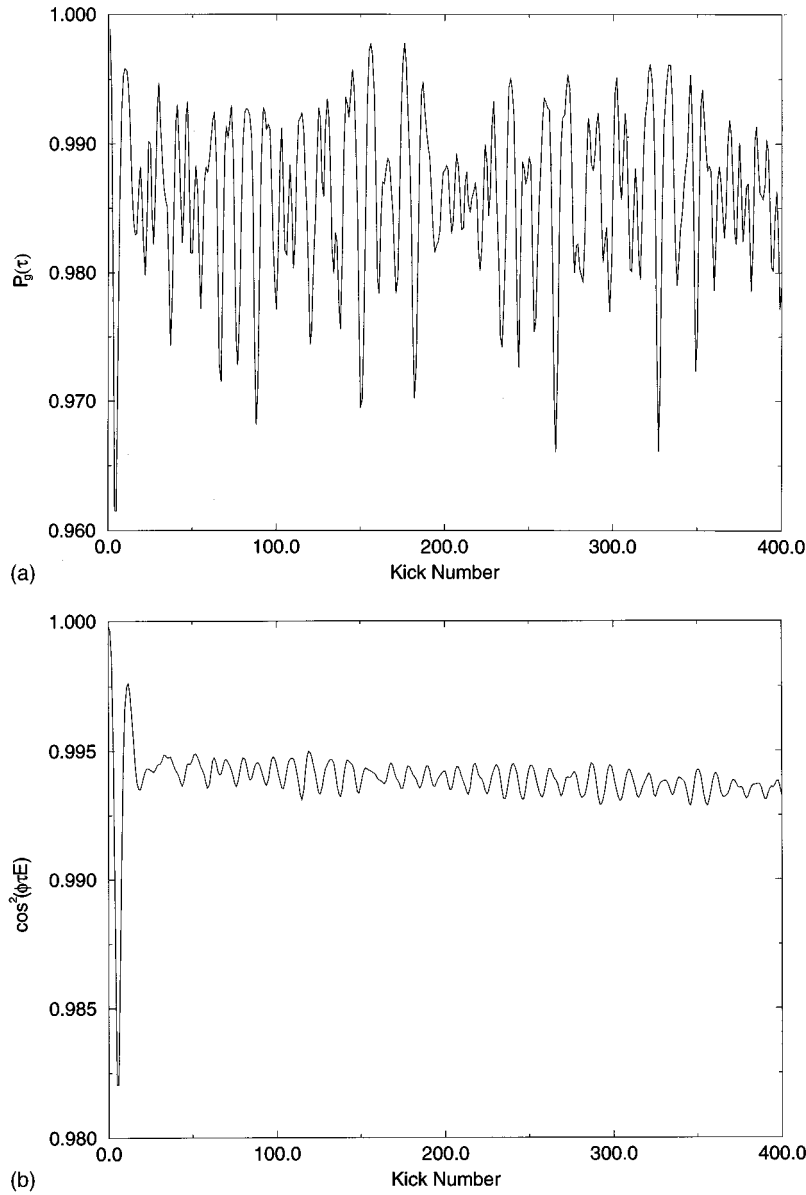
FIG. 4. Same as Fig. 3, except initial states are centered in a classically chaotic region, at $(1,0)$, with $g = 1.5$.

Raman pulse of duration T. In summary, we first prepare the ion electronic state by the application of a $\pi/2$ pulse and then apply the pulse at the carrier frequency, followed by the Raman parametric kick pulses. Pulses at the carrier frequency and the Raman pulses then alternate to effect each kick.

A particular advantage of this realization is that it is easy to read out the energy of the vibrational motion at any stage. If we do not reprepare the ion in the ground electronic state at the end of the carrier frequency pulse, its evolution will be dominated by the first term in Eq. (8). This is a QND measurement interaction for the vibrational quantum number. It causes the Bloch vector describing the two level system to precess around the x axis by an angle proportional to $a^\dagger a$. The probability of finding the atom in the ground state a time τ after the last squeezing pulse is

$$P_g(\tau) = \sum_{n=0}^{\infty} P(n)\cos^2\phi\tau n, \qquad (10)$$

where $\phi = \Omega\,\eta^2/2$. A set of readouts of the atomic state a time after an appropriate number of kicks thus enables a moment of the photon number to be constructed directly. This is similar to the scheme used by Meekhof *et al.* to observe the Jaynes-Cummings collapse and revival sequence [9].

In Figs. 3 and 4 we plot $P_g(\tau) = \langle \cos^2\phi\tau\hat{n}\rangle$ for the same two initial states and parameter values as discussed in Ref. [6]. In Fig. 3 the initial state is localized in a classically regular region of phase space. A regular collapse and revival sequence is evident in the quantum case [Fig. 3(a)]. In Fig. 4, however, we have the case of an initial state localized in the chaotic part of the classical phase space, leading to an irregular revival sequence. In both cases the corresponding classical moment is shown as well.

IV. DISCUSSION AND CONCLUSION

We can estimate reasonable values of the parameters θ, g, μ from recent experiments on trapped ions. From

Meekhof *et al.* [9], typical values are $\Omega = 10^6$, $\eta = 0.2$, and $g = 6$. For an interaction time of $T = 10$ μs, we have $\theta \approx 1.0$ and $\mu \approx 0.02$. It is then apparent that the parameter values of interest are achievable in an experiment.

However, the real limitation to observing the regular and irregular collapse and revival sequence is decoherence [6]. The departure of the quantum from the classical dynamics discussed in this paper is due to the preservation of quantum coherence between the eigenstates (Floquet states) of the kick operator. As these form a discrete set, the system must exhibit quasiperiodic behavior. The dynamics will depend on two things: (i) how many Floquet states make a significant contribution to the initial state and (ii) the commensurability of the Floquet eigenvalues. The primary reason why the chaotic case has such an irregular revival sequence is that the initial state has almost uniform support on the Floquet basis for these parameters. In both cases, however, the revivals are due to quantum coherence. Decoherence will thus be a problem.

There are two major sources of decoherence for this system. The first is spontaneous emission of the ion. In our scheme it is necessary to reprepare the ion in a superposition of the ground and excited states between each pulse. If the ion undergoes a spontaneous emission after this step the fu-

ture dynamics will not be described by our kick operators. However, this source of decoherence is not significant in current experiments as long-lived metastable levels are used. The other major source of decoherence is due to laser intensity and phase fluctuations. While this has not been definitely identified as the observed source of decoherence in current experiments, the decoherence that is observed is significant. The rate of decoherence between the ground and first excited state of the vibrational motion in [9] is quoted as of the order of 10 kHz. Comparing Figs. 3(a) and 3(b), we see that to observe a difference a kick number of about 100 must be reached. As the time between kicks is given by $T = 10$ μs, it is clear that a decoherence at this rate would most likely suppress the revival. The solution is to reduce the time between kicks by striving for a larger effective nonlinearity μ (by increasing laser power), while simultaneously decreasing the decoherence rate. If the dominant source of decoherence is laser intensity fluctuations there will be a trade-off between these two imperatives. However, while our scheme may be difficult to implement in present experiments, there is much more hope that the decoherence problem can be overcome in the ion realization than in a nonlinear optical realization.

[1] B. V. Chirikov, Phys. Rep. **52**, 263 (1979); G. M. Zaslavsky, *ibid.* **80**, 157 (1981).

[2] (a) M. Gutzwiller, *Chaos in Classical and Quantum Systems* (Springer, New York, 1990); (b) F. Haake, *Quantum Signatures of Chaos* (Springer, New York, 1990).

[3] R. Graham, M. Schlautmann, and P. Zoller, Phys. Rev. A **45**, R19 (1992).

[4] S. Dyrting and G. J. Milburn, Quantum Opt. **8**, 541 (1996).

[5] F. L. Moore, J. C. Robinson, C. Bharucha, P. E. Williams, and

M. G. Raizen, Phys. Rev. Lett. **73**, 2974 (1994).

[6] G. J. Milburn and C. A. Holmes, Phys. Rev. A **44**, 4704 (1991).

[7] C. A. Holmes, Phys. Lett. A **190**, 382 (1994).

[8] R. L. de Matos Filho and W. Vogel, Phys. Rev. Lett. **76**, 4520 (1996).

[9] D. Meekhof, C. Monroe, B. E. King, W. M. Itano, and D. J. Wineland, Phys. Rev. Lett. **76**, 1796 (1996).